

Concentration and Crystalline Phase Effects on the Spectroscopic Properties of Sol-Gel Synthesized Er³⁺:Y₂Si₂O₇ Nanopowders

Murat ERDEM¹, Hümeýra ÖRÜCÜ²

¹Marmara University, Faculty of Arts and Sciences, Physics Department, 34722, Istanbul

²Ege University, Faculty of Arts and Sciences, Physics Department, 35100, Izmir

(Alınış / Received: 28.09.2016, Kabul / Accepted: 07.12.2016, Online Yayınlanma / Published Online: 15.12.2016)

Keywords

Yttrium disilicate,
Nanophosphors,
Phase properties,
Sol-Gel

Abstract: Nanosized yttrium disilicate powders activated with trivalent erbium ions were produced by Sol-Gel known as wet chemical process. The structure and morphology of the synthesized powders were characterized by using X-ray diffraction spectroscopy (XRD), Transmission electron microscopy (TEM) and Photoluminescence spectroscopy. The XRD analysis revealed that the formation of triclinic α -Y₂Si₂O₇ and monoclinic β -Y₂Si₂O₇ polymorphs were obtained at 1050 °C and 1450 °C, respectively. The photoluminescence properties were also investigated in terms of sintering temperature and doping effect on different polymorphs.

Sol-Jel ile Sentezlenmiş Er³⁺:Y₂Si₂O₇ Nanofosforların Spektroskopik Özellikleri Üzerinde Konsantrasyon ve Faz Etkileri

Anahtar Kelimeler

İtiryum disilikat,
Nanofosfor,
Faz özellikleri,
Sol-Jel

Özet: Üç elektron değerlikli erbiyum iyonları ile katkılandırılmış nanoboyutlu İtiryum Silikat tozları yaş kimyasal bir yöntem olarak bilinen Sol-Jel ile üretilmişlerdir. Sentezlenen tozlar X-Işınları spektroskopisi (XRD), geçişli elektron mikroskopisi ve fotoluminesans spektroskopisi yöntemleri kullanılarak karakterize edilmişlerdir. XRD analizi sonuçlarında, 1050 °C ve 1450 °C de sentezlenen tozlar sırasıyla triklinik α -Y₂Si₂O₇ ve monoklinik β -Y₂Si₂O₇ kristal poliform yapılarını göstermiştir. Tavlama sıcaklığı ve farklı poliform yapılar üzerindeki katkılamanın etkisi bakımından fotoluminesans özellikleri ayrıca araştırılmıştır.

1. Introduction

Yttrium silicates (Y₂SiO₅ and Y₂Si₂O₇) are promising materials due to the electrical, magnetic and optical properties in the fields of photonics [1-5]. They are also ideal candidates for environmental barrier coating (EBC) and dental applications due to their excellent high temperature properties [6-10].

Yttrium disilicate (Y₂Si₂O₇) is one of the binary disilicates with high thermal and chemical stability (Melting point : 1775 °C), low dielectric constant, low linear coefficient of thermal expansion and low thermal conductivity. It shows γ , α , β , γ , and δ phases because of complex polymorphism resulting in comparative broad emission [11-12]. It is very difficult to obtain a pure phase of yttrium disilicate because of its intricate polymorphous structure.

Rare earth elements (RE) doped, co-doped and tri-doped Y₂Si₂O₇ are crucial nanophosphors for lasers, light emitting diodes (LED), white LED and plasma display panel applications [13-16]. Although, various rare earth-activated yttrium orthosilicates have been studied a lot [17-28], there have been a few studies reported on the Er³⁺ : Y₂Si₂O₇. Diaz et al. analyzed the luminescence properties of Y₂Si₂O₇ : Dy phosphors prepared by a new pressureless hydrothermal route. Their results indicated that the efficiency of Dy-doped β -Y₂Si₂O₇ phase is approximately 40% of that measured for the commercial phosphor Eu-Y₂O₃ [17]. Hreniak et al. studied the spectral output of Y₂Si₂O₇ : Tb, Y₂Si₂O₇ : Er, Yb and Y₂Si₂O₇ : Pr, Yb glass, thin film and phosphor materials synthesized by the sol-gel method. They have found that the luminescence properties and lifetimes depend strongly on annealing temperature [18-19]. Zhou et al. synthesized the nanocrystalline Y₂Si₂O₇ : Eu phosphors with an average size of 60 nm using silica

aerogel as raw material. Compared with Y₂O₃/SiO₂ crystalline, they declared that the excitation and emission peaks of nanocrystalline red-shifted and led to enhance of its luminescence intensity [20]. Li et al. synthesized Y₂Si₂O₇: Eu, Y₂Si₂O₇: Tb and Y₂Si₂O₇: Ce, Tb phosphors via sol-gel method. They focused on energy transfer mechanisms between Tb³⁺ and Ce³⁺ ions and discussed photoluminescence intensity on Re³⁺ concentration in detail [21-22]. Thanh et al. studied the structure of Y₂Si₂O₇: Ce phosphors prepared by the sol-gel method with added ammonia. The blue light was emitted when excited by the 325 nm UV radiation [23].

Sokolnicki investigated the upconversion luminescence from Er³⁺ in nanocrystalline Y₂Si₂O₇: Er and Y₂Si₂O₇: Yb, Er and produced Y₂Si₂O₇: Ce, Eu, Tb phosphors by combustion and sol-gel techniques. The white light emission is obtained by varying the concentration of the active ions and treating atmosphere [14, 24]. Marciniak et al. presented the spectroscopic properties of Y₂Si₂O₇: Er³⁺ nanocrystalline powder and thin film synthesized by the sol-gel method [25].

In our former studies, we have discussed the structural and spectroscopic properties of Y₂Si₂O₇: Nd and Y₂Si₂O₇: Yb phosphors [26, 27] and the up-conversion properties of Y₂Si₂O₇: Yb, Er nanophosphors obtained by sol-gel technique [28].

In the present study structural characterization and the spectroscopic properties of Er³⁺ doped nanocrystalline yttrium disilicate samples fabricated using sol-gel method are reported depend upon crystalline phase properties. Due to the efficient luminescence properties at the telecommunication wavelength of 1.54 μm, Erbium doped materials have received considerable interest in optical amplifiers and silicon photonics [15, 29].

2. Material and Method

Er³⁺: Y₂Si₂O₇ nanopowders were synthesized in the phase diagram of SiO₂-Y₂O₃ binary system using the sol-gel method to obtain two different phases. TEOS (Si (OC₂H₅)₄) with 99.9% purity, yttrium nitrate (Y (NO₃)₃ · 6H₂O), and erbium nitrate (Er (NO₃)₃ · 5H₂O) salts with 99.9% purity were used to produce the nanopowders. Detail explanation of the fabrication process could be reached in our recent study [28]. The fabricated samples were then annealed at 1050 °C and 1450 °C for 12 hours to produce nanocrystalline Y₂Si₂O₇ powders. Three different samples were synthesized with 0.5, 1.0, 1.5 mol % ratios for Er³⁺ ions; they were labeled as YSE1, YSE2, YSE3, respectively.

The structural properties of two powders were conducted using X-ray diffraction spectroscopy (Model of Rigaku-XRD 2200 D/MAX) with the Cu-Kα source operated with the wavelength at λ = 1.5418 Å.

Slit systems, step-size (0.02°), source voltage (40 kV), and current (30 mA) were kept constant during the scans that were conducted in θ-2θ coupled mode. The morphological properties of the powders were also investigated by TEM with model number JEOL JEM-2100.

The photoluminescence (PL) spectrums of all powders were conducted using a diode laser (Laser Drive Inc.-LDI-820) with a wavelength of 800 nm. The emissions resulting from the dopant ions of the powders were transmitted to a Monochromator (McPherson Inc. Model 2051) and measured by an InGaAs semiconductor detector (Princeton Inc. Model ID-441-C) with a preamplifier (Stanford Res. Model SR560). A short wavelength pass filter (800 nm) was placed in front of the monochromator to eliminate the scattering lights in the measurements.

The decay measurements of the dopant ions in the powders under pulsed excitation were taken by using the titanium sapphire laser (Model of Schwarz Electro-Optics Inc. Titan-P) and a digital oscilloscope (Model of Tektronix- TDS3052B). All spectral output of the nanopowders was recorded at room temperature.

3. Results and Discussion

3.1. X-ray diffraction analysis

The phase evolution of the phosphors heat-treated at different temperatures was determined using X-ray diffraction analysis. The XRD patterns of the Er³⁺ doped Y₂Si₂O₇ (YSE1, YSE2 and YSE3) samples calcined at two different temperatures are shown in Figure 1.

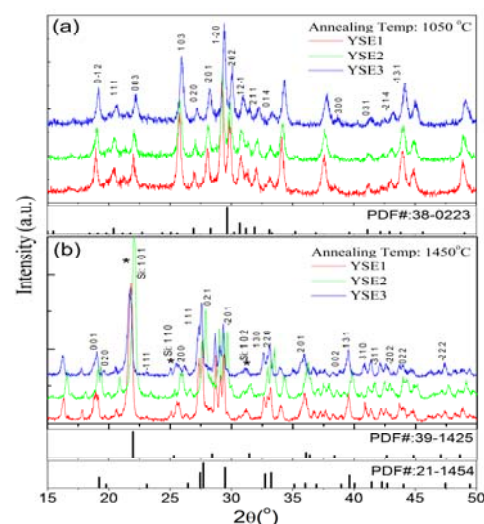


Figure 1. The X-ray patterns of YSE powders calcined at (a) 1050 °C, (b) 1450 °C.

It can be seen in Figure 1a, 1b that α-Y₂Si₂O₇ (JCPDS file no. 38-0223) is the dominant (main) phase for the Er³⁺ doped powders calcined at 1050 °C. Annealing the samples to 1450 °C resulted in the growth of the

β -Y₂Si₂O₇ crystalline phase which is well consistent with the JCPDS file no. 21-1454. We observed also the presence of the SiO₂ (JCPDS file no. 39-1425) peak located at $2\theta = 22^\circ$ (indicated with an asterix * in Figure 1b). Similar results have been recently reported by Becerro et al and Diaz et al. [30, 31]. The structure of the other phases and the intensity of the peaks do not change as a function of Er³⁺ doping concentration, indicating that the doping ions do not contribute to the formation of new phases.

The polymorphs of yttrium disilicates transform from one phase into another with increasing temperature [32]. However, phase transition temperatures vary considerably in the studies of different researchers [17, 18, 33, 34]. This demonstrates that the yttrium disilicate structure is strongly dependent on the synthesis methods, annealing temperatures and pressure.

3.2. Transmission electron microscopy results

Morphological properties and the particle size distribution of calcined powders were identified with transmission electron microscope. Figure 2 illustrates the TEM images of 1.0% Er³⁺ doped yttrium disilicate samples (YSE2) annealed at 1050 °C and 1450 °C. The yttrium disilicate powders have regular crystalline form and the particle size of crystallites increase with the increasing annealing temperatures. The average size of nano particles estimated from TEM images is about ~100 nm for α -Y₂Si₂O₇, and 0.5 μ m for β -Y₂Si₂O₇.

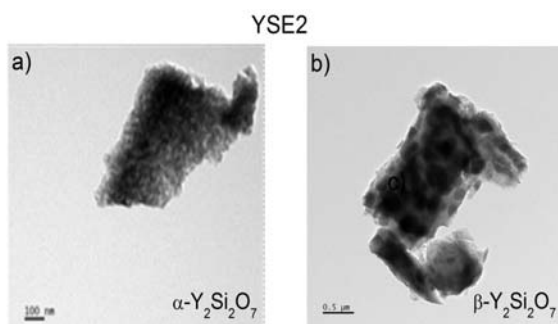


Figure 2. The TEM images of 1.0% Er³⁺ doped yttrium disilicate samples (YSE2) annealed at (a) 1050 °C, (b) 1450 °C.

3.3. Photoluminescence (PL) properties

Figure 3 shows the spectral output of photoluminescence measurement of Er³⁺:Y₂Si₂O₇ nanopowders in the 1425-1675 nm wavelength range at room temperature when excited with diode laser operating at 800 nm. The spectral intensity of the lines and band broadening of the spectral output decreased with the increase of Er³⁺ mole concentration (Fig. 3a, 3b). The sample doped with 1.0 mole % Er³⁺ ions portrayed higher luminescence intensity than the other concentrations of Er³⁺ ions for each phase. The change in intensity with Er³⁺

concentration could be on account of the interaction among the Er³⁺ ions causing the energy transfer mechanisms.

Each spectrum contains an emission band with the strongest emission peak at about 1550 nm which correspond to the transition from the ⁴I_{13/2} to the ground level (⁴I_{15/2}), within the 4f shell of the Er³⁺ ions. The J-manifolds of Er³⁺ ions are split due to the low symmetry (C₁ or C₂) of the Y₂Si₂O₇ cation sites [25]. We observed that the spectral form and the count of the Stark components showed similar behavior for each Er³⁺ ions transitions in the powders at each phase. This phenomenon can be ascribed to the crystal field effect of ligand ions surrounding the Er³⁺ ions due to the same crystalline phase.

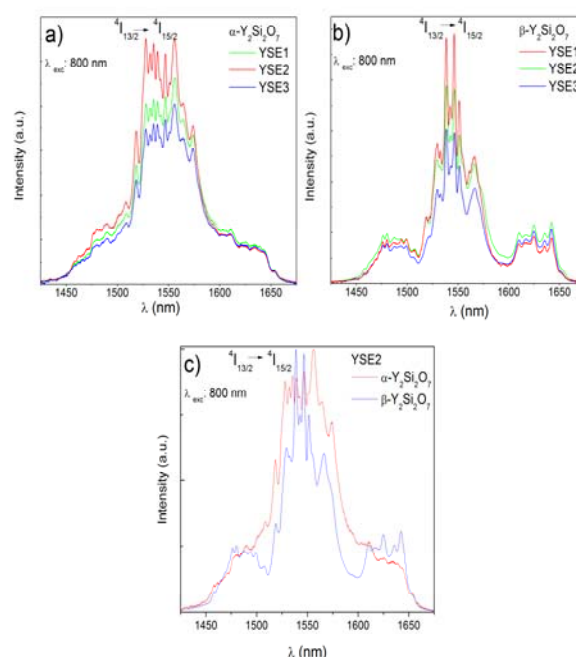


Figure 3. (a,b) The spectral output of luminescence measurement of Er³⁺:Y₂Si₂O₇ nanopowders in the 1425-1675 nm wavelength range at room temperature, (c) the comparison of emission bands for α - and β - Er³⁺:Y₂Si₂O₇ 1% phases.

Figure 3c presents the comparison of emission bands for α and β - Er³⁺:Y₂Si₂O₇ 1% phases. The spectral output of Er³⁺ emission shows strong dependency of the crystalline phase.

All these results can be attributed to the varied numbers of Y³⁺ (Er³⁺) sites in the structures. In β -phase has one Y³⁺ site with C₂ symmetry and in α -phase there are four different Y³⁺ sites with C₁ symmetry. Er³⁺ ions can substitute in four different crystallographic sites of Y³⁺ ions in α -phase and emission from these four sites can occur in the widening of the emission band. Thus, the spectral output of the emission indicates a more significant difference of the silicate crystalline phase for Er³⁺ ions [25].

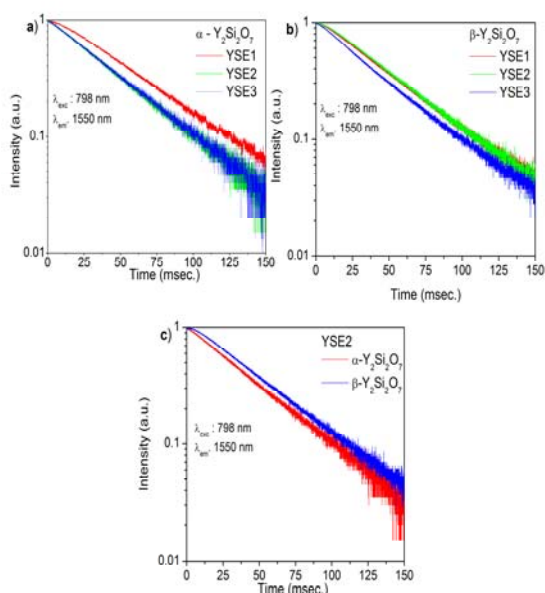


Figure 4. (a,b) The decay curves of the $4I_{13/2}$ level for all samples under excitation wavelength of 798 nm at room temperature, **(c)** the comparison of decay curves for α - and β - Er³⁺:Y₂Si₂O₇ 1% phases.

The decay curves of the $4I_{13/2}$ level have been measured for all samples excitation wavelength of 798 nm at room temperature. Figure 4 represents the decay plots in semi-log scale for three powders. The decay time of the $4I_{13/2}$ emission decreases with increasing Er³⁺ mole concentration in the crystalline powders (Fig. 4a, 4b). The comparison of the PL decay curves of YSE2 sample in the three crystalline phases has been shown in Fig. 4c. All these decay curves of α - and β -phases have similar lifetime values.

4. Conclusion

α -Y₂Si₂O₇ and β -Y₂Si₂O₇ phosphors were successfully synthesized by sol-gel route using yttrium nitrate, erbium nitrate salts, TEOS (Si (OC₂H₅)₄) and hydrochloric acid as a catalyst for the hydrolysis of TEOS as the starting materials. The structure and the phase purity of the powders are determined by XRD and TEM analysis. α - and β -phases of crystalline Er³⁺:Y₂Si₂O₇ phosphors were obtained via changing thermal treatment process.

The influences of crystalline phase on the spectral profile of Er³⁺:Y₂Si₂O₇ phosphors were studied in detail. Although doping of rare earth ion amounts do not contribute to the phase evolution of the powders, it is observed that the spectroscopic properties depend strongly on phase properties of Y₂Si₂O₇. We also observed that Y₂Si₂O₇ : Er³⁺ 1.0 mol % showed higher PL intensity for each phase than the other concentrations of Er³⁺ ions.

Acknowledgments

The authors would like to thank Prof. Dr. Baldassare Di Bartolo for his valuable support.

References

- [1] Pennenvan R.A., Rosenzweig, R.R. 1973. 13, 99–199. Structure and bonding. Volume 13, 1973, Rare earths Berlin : Springer, 13, 99-199.
- [2] Becerro, A.I., Escudero, A., Florian, P., Massiot, D., Alba, M.D. 2004. Revisiting Y₂Si₂O₇ and Y₂SiO₅ polymorphic structures by ⁸⁹Y MAS-NMR spectroscopy. J. Solid State Chem 177, 2783–2789.
- [3] Cao, M.S., Hou, Z.L., Yuan J.L., Xiong, L.T., Shi, X.L. 2009. Low dielectric loss and non-Debye relaxation of gamma-Y₂Si₂O₇ ceramic at elevated temperature in X-band. J. Appl. Phys. 105, 2–5.
- [4] Ching, W.Y., Ouyang, L., Xu, Y.N. 2003 Electronic and optical properties of Y₂SiO₅ and Y₂Si₂O₇ with comparisons to α -SiO₂ and Y₂O₃. Phys. Rev. B 67, 245108.
- [5] Wang, G.M., Equall, R.W., Cone, R.L., Leask, M.J.M., Godfrey, K.W., Wondre, F.R. 1996. Optical dephasing mechanisms in Tm³⁺:Y₂Si₂O₇. Opt. Lett. 21, 818–820.
- [6] Moya, J.S., Diaz, M., Serna, C.J., Castanho, S.M. 1998. Formation of nanocrystalline yttrium disilicate powder by an oxalate gel method J. Eur. Ceram. Soc. 18, 1–4.
- [7] Zheng X.H., Du, Y.G., Xiao J.Y., Zhang, W.J., Zhang, L.C. 2009. Double layer oxidation resistant coating for carbon fiber reinforced silicon carbide matrix composites Appl. Surf. Sci. 255, 4250–4254.
- [8] Diaz, M., Cano, I.G., Castanho, S.M., Moya, J.S., Rodríguez, M.A. 2001. Synthesis of nanocrystalline yttrium disilicate powder by a sol-gel method J. Non. Cryst. Solids. 289, 151–154.
- [9] Seifert, H.J., Wagner, S., Fabrichnaya, O., Lukas, H.L., Aldinger, F.L., Ullmann, T., Schmucker, M.; Schneider, H. 2005. Yttrium Silicate Coatings on Chemical Vapor Deposition-SiC-Precoated C/C-SiC: Thermodynamic Assessment and High-Temperature Investigation. J. Am. Ceram. Soc., 88, 424–430.
- [10] Stoner, B.R., Griggs, J.A., Neidigh, J., Piascik, J.R. 2014. Evidence of yttrium silicate inclusions in YSZ-porcelain veneers. J. Biomed. Mater. Res. Part B Appl. Biomater. 102, 441–446.
- [11] Sun, Z., Zhou, Y., Wang, J., Li, M. 2008. Thermal Properties and Thermal Shock Resistance of γ -Y₂Si₂O₇. J. Am. Ceram. Soc. 91, 2623–2629.
- [12] Hu, H.; Zeng, Y.; Zuo, K.; Xia, Y.; Yao, D.; Günster, J.; Jürgen G.; Heinrich, S.L. 2015. Synthesis of porous Si₃N₄/SiC ceramics with rapid nitridation of silicon. J. Eur. Cer. Soc. 35, 3781–3787.
- [13] Deng, Y., Song, W.; Dong, W., Dai, R., Wang, Z., Zhang, Z., Ding, Z. 2014. White light emission of Eu³⁺/Ag co-doped Y₂Si₂O₇. J. Rare Earths. 32, 779–786.

- [14] Sokolnicki, J. 2013. Rare earths (Ce, Eu, Tb) doped Y₂Si₂O₇ phosphors for white LED. 2013. *J. Lumin.* 134, 600–606.
- [15] Wang, B., Wang, X.J., a De Dood, M.J., Guo, R.M., Wang, L., Vanhoutte, M., Michel, J., Kimerling, L.C., Zhou, Z. 2012. Photoluminescence quantum efficiency and energy transfer of ErRE silicate (RE = Y, Yb) thin films. *J. Phys. D. Appl. Phys.* 45, 165101-165106.
- [16] Hreniak, D., Głuchowski, P., Stręk, W., Bettinelli, M., Kozłowska, A., Kozłowski, M. 2006. Preparation and upconversion properties of Er³⁺, Yb³⁺:Y₂Si₂O₇ nanocrystallites embedded in PVA polymer nanocomposites. *Mater. Sci. Poland.* 24, 405-412.
- [17] Diaz, M., Pecharroman, C., Del Monte, F., Sanz, J., Iglesias, J.E., Moya, J.S., Yamagata, C., Mello-Castanho, S. 2005. Synthesis, Thermal Evolution, and Luminescence Properties of Yttrium Disilicate Host Matrix. *Chem. Mater.* 17, 1774–1782.
- [18] Hreniak, D., Stręk, W., Opalińska, A., Nyk, M., Wołczyr, M., Lojkowski, W., Misiewicz, J. 2004. Luminescence Properties of Tb-Doped Yttrium Disilicate Prepared by the Sol-Gel Method. *J. Sol-Gel Sci. Technol.* 32, 195–200.
- [19] Grzeszkiewicz, K., Marciniak, L., Stręk, W., Hreniak, D. 2016. Downconversion in Y₂Si₂O₇: Pr³⁺, Yb³⁺ polymorphs for its possible application as luminescent concentrators in photovoltaic solar-cells. *J. Lumin.* 177, 172-177.
- [20] Zhou, P., Yu, X., Yang, L., Yang, S., Gao, W. 2004. Synthesis of Y₂Si₂O₇:Eu nanocrystal and its optical properties. *J. Lumin.* 124, 241–244.
- [21] Li, Y., You, B., Zhao, W., Zhang, W., Yin, M. Chinese. 2008. Synthesis and Luminescent Properties of Nano-scale Y₂Si₂O₇:Re³⁺ (Re=Eu, Tb) Phosphors via Sol-Gel Method. *J. Chem. Phys.* 21, 376–380.
- [22] Li, Y., Wei, X., Yin, M., Tao, M. 2011. Energy transfer processes in Ce³⁺ and Tb³⁺ co-doped Ln₂Si₂O₇ (Ln = Y, Gd). *Opt. Mater.* 33, 1239–1242.
- [23] Thanh, L.X., Phuong, P.T.M. 2012. A Study of Synthesis of Cerium-Doped Yttrium Silicate and Yttrium Disilicate Phosphors by the Ammonia-Added Sol-Gel Method. *E-Journal Surf. Sci. Nanotech.* 10, 248–251.
- [24] Sokolnicki, J. 2011. Upconversion luminescence from Er³⁺ in nanocrystalline Y₂Si₂O₇:Er³⁺ and Y₂Si₂O₇:Yb³⁺, Er³⁺ phosphors. *Mater. Chem. Phys.* 131, 306–312.
- [25] Marciniak, L., Hreniak, D., Stręk, W., Piccinelli, F., Speghini, A., Bettinelli, M., Miritello, M., Lo Savio, R., Cardile, P., Priolo, F. 2016. Spectroscopic and structural properties of polycrystalline Y₂Si₂O₇ doped with Er³⁺. *J. Lumin.* 170, 614–618.
- [26] Erdem, M., Eryürek, G., Mergen, A., Di Bartolo, B. 2016. Pressure effects on the cooperative emission of Yb³⁺: Y₂Si₂O₇ nano-powders. *Ceram. Int.* 42, 1501–1506.
- [27] Erdem, M., Özen, G., Tav, C.; Di Bartolo, B. 2013. Structural and Spectroscopic Properties of δ-Y₂Si₂O₇ Nanopowders Activated with Nd³⁺ Ions. *Ceram. Int.* 39, 6029–6033.
- [28] Erdem, M., Sitt, B. 2015. Up conversion based white light emission from sol-gel derived α-Y₂Si₂O₇ nanoparticles activated with Yb³⁺, Er³⁺ ions. *Opt. Mater.* 46, 260–264.
- [29] Najar, A. Omi, H., Tawara, T. 2014. Scandium effect on the luminescence of Er-Sc silicates prepared from multi-nanolayer films. *Nanoscale Res. Lett.* 9, 356.
- [30] Becerro, A., Naranjo, M., Pedrigón, A., Trillo J. 2003. Hydrothermal chemistry of silicates: Low-temperature synthesis of γ-yttrium disilicate. *J. Am. Ceram. Soc.* 86, 1592–1594.
- [31] Becerro, A.I., Naranjo, M., Alba, M.D., Trillo, J.M. 2003. Structure-directing effect of phyllosilicates on the synthesis of γ-Y₂Si₂O₇. Phase transitions in Y₂Si₂O₇. *J. Mater. Chem.* 13, 1835-1842.
- [32] Ito, J., Johnson, H. 1968. Synthesis and study of yttrilite. *The American Mineralogist*, 1968, 53, 1940-1952.
- [33] Erdem, M., Eryürek, G., Di Bartolo, B. 2015. White light emission from sol-gel derived γ-Y₂Si₂O₇ nanoparticles. *J. Alloys Compd.* 639, 483–487.
- [34] Marciniak, L., Hreniak, D., Dobrowolska, A., Zych, E. 2010. Size-dependent luminescence in Y₂Si₂O₇ nanoparticles doped with Ce³⁺ ions. *Appl. Phys. A Mater. Sci. Process.* 99, 871–877.